VIBROACOUSTIC ANALYSIS OF CYCLIC STRUCTURES

Abdelkhalak El hami
INSA de Rouen, LMR, 76801 St Etienne du Rouvray, France
aelhami@insa-rouen.fr

Dan Borza
INSA de Rouen, LMR, 76801 St Etienne du Rouvray, France
borza@insa-rouen.fr

José Eduardo Souza de Cursi
INSA de Rouen, LMR, 76801 St Etienne du Rouvray, France
souza@insa-rouen.fr

Abstract: *We propose a method for the vibroacoustic analysis of structures having symmetry properties. This method is based on the reduction of the number of the degrees of freedom involved (size reduction) and the use of experimental data (confrontation numerical / experimental). We propose the extension of the method of the linear representations of finite symmetry groups to problems of coupling fluid-structure. This approach leads to a significant reduction of the number of degrees of freedom, with a maximal reduction for the so called repetitive structures, but keeps the quality of the approximations. Finally, we present a practical case of the modal analysis – in air and water - of a ship propeller formed by 3 steel Stainless pales. The experimental results are obtained by using the whole-field, non-contact technique of electronic holography.*

Keywords: Vibroacoustics, modal analysis, model reduction, holography, symmetry groups

1. Introduction

Manufacturers are interested in forecasts concerning the dynamical behavior of structures, since improvements in the lifetime, security, comfort or global performance may be obtained by determining unacceptable levels of vibration and protecting their products against these ones.

In the particular case of hydraulic turbines, ribbed shells, aerospatial structures, such a analysis is considered as crucial since these structures are submitted to a wide number of sources of vibration, what increases the risks of failure and nuisance. In this case, the models used must take into account the operating conditions, where the structure is immersed into a dense fluid (air or water).

The modal analysis of complex structures by Finite Element Methods (FEM) involves generally a large number of degrees of freedom (DOF). When the coupling with a fluid is considered, this large number is already increased by the addition of the DOF corresponding to the fluid domain. In order to perform an appropriate computational analysis, the reduction of the size of the resulting matrices (i. e., the reduction of the number of DOF) is generally compulsory.

For linear structures presenting symmetry of repetitive type, the theory of finite symmetry groups furnishes tools which allow such a reduction without a significant loss of precision: the size reduction keeps the quality of the approximation. This work is a step for the extension of these approach to the dynamical analysis of a rotating cyclic elastic structure immersed into a dense fluid - what is the case of the mechanical structures mentioned above. We focus on the vibroacoustic analysis and the determination of the modal basis of the structure immersed in the same fluid at the rest: we examine the coupled fluid-structure system for the range of frequencies where the added mass effects are dominating (low frequency region) and linear behavior may be assumed. This situation corresponds to a large part of the industrial applications. By limitation of the room, we do not present here the theory of symmetry groups and we focus on its application to the coupled fluid-structure situation and the significant reduction of the number of DOF which is obtained. We present a practical example concerning the modal analysis of a ship propeller.

2. Finite symmetry groups and reduction of the number of DOF

The proposed approach for the vibroacoustic analysis of a cyclic structure involves two steps: initially, the application of the theory of finite symmetry groups and modal synthesis technique lead to a reduced model. Then, the vibroacoustic behavior of the cyclic structure is analyzed by using the reduced model. In this section, we detail the first step. We assume that the structure presents a repetitive cyclical geometry and that the FEM mesh used is also repetitive.

Thus, the structure is formed of a set of NS identical substructures (also called cells) and the FEM mesh of each substructure is identical. So, the mass and stiffness matrices associated to each substructure are also identical:

$$M_S^{(1)} = ... = M_S^{(NS)} = M \; ; \qquad K_S^{(1)} = ... = K_S^{(NS)} = K$$

In order to reduce the model, we decompose all the quantities in their boundary and interior components: for the substructure number k,

$$M = \begin{bmatrix} M_{cc} & M_{ci} \\ M_{ic} & M_{ii} \end{bmatrix} \; ; \quad K = \begin{bmatrix} K_{cc} & K_{ci} \\ K_{ic} & K_{ii} \end{bmatrix} \; ; \quad U^{(k)} = \begin{bmatrix} U_c^{(k)} \\ U_i^{(k)} \end{bmatrix} \; ; \quad F^{(k)} = \begin{bmatrix} F_c^{(k)} \\ F_i^{(k)} \end{bmatrix} \tag{1}$$

where $U^{(k)}$ is the field of displacements and $F^{(k)}$ are the external forces. The index i refers to interior quantities and the index c to the boundary ones. In the general situation, $U^{(k)}$ is different for each cell, since $F^{(k)}$ may be different for each one. The forces applied by the other substructures on the substructure k are boundary forces and appear in F_c. In the sequel, since no ambiguity is involved, we drop the index k anywhere it is not necessary.

Under cyclic symmetry, the subsystems takes the geometrical form of circular sectors and the boundary forces are usually decomposed in "left" and "right" components and we have (the index k is dropped):

$$M = \begin{pmatrix} M_{11} & M_{12} & M_{13} \\ M_{21} & M_{22} & M_{23} \\ M_{31} & M_{32} & M_{33} \end{pmatrix} \; ; \quad K = \begin{pmatrix} K_{11} & K_{12} & K_{13} \\ K_{21} & K_{22} & K_{23} \\ K_{31} & K_{32} & K_{33} \end{pmatrix} \; ; \quad U = \begin{pmatrix} U_L \\ U_R \\ U_I \end{pmatrix} \; ; \quad F = \begin{pmatrix} F_L \\ F_R \\ F_I \end{pmatrix} \tag{2}$$

2.1 Reduction in the static case

The equilibrium of each cell is described by $KU = F$, where the external forces are $F_L = f_L + f_L^{ext}$, $F_R = f_R + f_R^{ext}$, $F_I = f_I^{ext}$. $f_L^{ext}, f_R^{ext}, f_I^{ext}$ are the left, right and interior components of the external forces applied to the cell; f_L, f_R are the left, right forces applied by the other substructures to the cell (internal forces). The compatibility relations concerning the displacements and forces at the interfaces between yield

$$U_R^{(k)} = e^{ika} U_L^{(k)} \; ; \quad f_R^{(k)} = -e^{ika} f_L^{(k)} \; ; \quad a = 2\pi/NS \; ; \quad i^2 = -1 \; ; \quad k=1, ...NS. \tag{3}$$

$$(f_L^{ext}, f_R^{ext}, f_I^{ext})^{(k)} = \frac{1}{NS} \sum_{j=1}^{NS} \left(f_j^{ext} e^{-ijak} \right) \tag{4}$$

$U_R^{(k)}$ is eliminated either by an energetic method employing the Lagrange equations or by a penalty method. The complex system becomes:

$$\begin{bmatrix} K_{11} + K_{22} + e^{ika} K_{12} + e^{-ika} K_{21} & K_{13} + e^{-ika} K_{23} \\ K_{31} + e^{ika} K_{32} & K_{33} \end{bmatrix} \begin{bmatrix} U_L \\ U_I \end{bmatrix}^{(k)} = \begin{bmatrix} f_L^{ext} + e^{ika} f_R^{ext} \\ f_I^{ext} \end{bmatrix}$$

By writing $U_L = U_L^r + i U_L^I$; $U_I = U_I^r + i U_I^I$; $\alpha = ka$, this equation becomes:

$$\begin{pmatrix} \widetilde{\widetilde{K}}_{11} & \widetilde{\widetilde{K}}_{12} \\ -\left(\widetilde{\widetilde{K}}_{12}\right)^t & \widetilde{\widetilde{K}}_{22} \end{pmatrix}^{(k)} \begin{pmatrix} U_L^r \\ U_I^r \\ U_L^I \\ U_I^I \end{pmatrix}^{(k)} = \begin{pmatrix} f_L^{ext} + \cos(\alpha) f_R^{ext} \\ f_I^{ext} \\ \sin(\alpha) f_R^{ext} \\ 0 \end{pmatrix}^{(k)} \tag{5}$$

$$\widetilde{\widetilde{K}}_{11} = \begin{bmatrix} K_{11} + K_{22} + \cos(\alpha)(K_{12} + K_{21}) & K_{13} + \cos(\alpha) K_{23} \\ K_{13} + \cos(\alpha) K_{32} & K_{33} \end{bmatrix} \; ; \; \widetilde{\widetilde{K}}_{22} = \widetilde{\widetilde{K}}_{11} \tag{6}$$

$$\widetilde{\widetilde{K}}_{12} = \begin{bmatrix} -\sin(\alpha)(K_{12} - K_{21}) & \sin(\alpha) K_{23} \\ -\sin(\alpha) K_{32} & 0 \end{bmatrix} \tag{7}$$

At each cell, the solution Re(U_j) is given by U =(U^r, U^I)^t, where

$$(U^r = (U^r_G, U^r_I)^t, \quad (U^I = (U^I_G, U^I_I)^t \text{ and } U^r_G = Re(e^{ia}U_D), \quad U_j = \sum_{h}^{NS}(U^{(j)})^t e^{iajh} \tag{8}$$

2.2 Reduction in the dynamical situation

The dynamical equilibrium of each substructure reads as MU + KU = F. At first, we determine a basis associated to the boundary DOF. Then, the basis is completed in order to describe the whole structure.

a) **Basis associated to the boundary DOF** : Since linearity is assumed, static interior displacements are a linear function of the static boundary ones: $U_i = \Phi_c U_c$. The matrix Φ_c may be determined as follows: let b be the index describing a boundary DOF. When a unitary displacement is imposed to this single DOF ($U_{c,b} = 1$; $U_{c,n} = 0$ for $n \neq b$), the corresponding vector $\Phi_{i,b}$ of displacements of the interior DOF is determined by solving the static problem previously considered. Φ_c is the matrix formed by assembling these vectors. Φ_c is the basis of the n_m first modes of the problem. The quality of the approximations in this basis is connected to the value of the fundamental eigenfrequency $f_{c,0}$ corresponding to clamping boundary conditions ($U_{c,n} = 0$ for any n, including $n= b$). In practice, the index n_m corresponds to the index of $f_{c,0}$ in the list of the natural frequencies and the basis is used in the range of frequencies $\left[0, f_{c,0}/3 \right]$.

b) **Construction of a complete basis** : Let us introduce a new basis

$$\begin{bmatrix} U_c \\ U_i \end{bmatrix} = \begin{bmatrix} I & O \\ \Phi_c & \Phi_i \end{bmatrix} \begin{bmatrix} U_c \\ P_i \end{bmatrix}$$

yielding the condensed matrices :

$$\begin{cases} \widetilde{\widetilde{K}}_{cc} = K_{cc} + K_{ci}\Phi_c \\ \widetilde{\widetilde{K}}_{ic} = \left(\widetilde{\widetilde{K}}_{ci}\right)^t = 0 \\ \widetilde{\widetilde{K}}_{ii} = \Phi_i^t K_{ii}\Phi_i = \Lambda_i \end{cases} \qquad \begin{cases} \widetilde{\widetilde{M}}_{cc} = M_{cc} + \Phi_c^t M_{ic} + M_{ci}\Phi_c + \Phi_c^t M_{ii}\Phi_c \\ \widetilde{\widetilde{M}}_{ci} = \left(\widetilde{\widetilde{M}}_{ic}\right)^t = M_{ci}\Phi_i + \Phi_c^t M_{ii}\Phi_i \\ \widetilde{\widetilde{M}}_{ii} = \Phi_i^t M_{ii}\Phi_i = I \end{cases} \tag{9}$$

Analogously to the static situation, the following system is solved for each cell:

$$\left[\begin{pmatrix} K_{11}K_{12}K_{13} \\ K_{21}K_{22}K_{23} \\ K_{31}K_{32}K_{33} \end{pmatrix} - \omega_2 \begin{pmatrix} M_{11}M_{12}M_{13} \\ M_{21}M_{22}M_{23} \\ M_{31}M_{32}M_{33} \end{pmatrix} \right]^{(k)} \begin{pmatrix} U_L \\ U_R \\ U_I \end{pmatrix}^{(k)} = \begin{pmatrix} f_L \\ f_R \\ f_I \end{pmatrix}^{(k)} \tag{10}$$

The calculation is similar to the static case but no exterior forces are applied. Due to the symmetry of the problem, only the (NS/2+1) sub problems need to be solved. For each α (the f_I are zero).

$$\left[\widetilde{\widetilde{K}}(\alpha) - \omega^2 \widetilde{\widetilde{M}}(\alpha) \right] \widetilde{\widetilde{U}} = 0 \tag{11}$$

where $\alpha \in \{\pi/NS, 4\pi/NS, ..., \pi n/NS\}$. If NS is even, n = NS/2 and if NS is odd n = (NS-1)/2.

$$\widetilde{\widetilde{K}}(\alpha) = \begin{pmatrix} \widetilde{\widetilde{K}}_{11} & \widetilde{\widetilde{K}}_{12} \\ -\left(\widetilde{\widetilde{K}}_{12}\right)^t & \widetilde{\widetilde{K}}_{11} \end{pmatrix} \qquad \widetilde{\widetilde{M}}(\alpha) = \begin{pmatrix} \widetilde{\widetilde{M}}_{11} & \widetilde{\widetilde{M}}_{12} \\ -\left(\widetilde{\widetilde{M}}_{12}\right)^t & \widetilde{\widetilde{M}}_{11} \end{pmatrix} \tag{12}$$

$\widetilde{\widetilde{K}}_{11}$ and $\widetilde{\widetilde{K}}_{12}$ are given by Eqs. (6)-(7). $\widetilde{\widetilde{M}}_{11}$ and $\widetilde{\widetilde{M}}_{12}$ have analogous definitions:

$$\widetilde{\widetilde{M}}_{11} = \begin{bmatrix} M_{11} + M_{22} + \cos(\alpha)(M_{12} - M_{21}) & M_{13} + \cos(\alpha)M_{23} \\ M_{31} + \cos(\alpha)M_{32} & M_{33} \end{bmatrix} \tag{13}$$

$$\widetilde{\widetilde{M}}_{12} = \begin{bmatrix} -\sin(\alpha)(M_{12} - M_{21}) & \sin(\alpha)M_{23} \\ -\sin(\alpha)M_{32} & 0 \end{bmatrix} \tag{14}$$

The modes of the global structure are expanded for a given calculated frequency, using the corresponding vector

$$U = \text{Re}\left\{\left(\widetilde{U}, \ e^{ia}\widetilde{U}, \ e^{i2a}\widetilde{U}, ..., \ e^{i(NS-1)a}\widetilde{U}\right)^t\right\} \tag{15}$$

A demonstration of this expansion is given in (El Hami,A and Radi,B. 1996). This approach requires a reduced storage: only the stiffness matrix of the cell is needed. It also saves calculation times by the use of the reduced problem. The validity of proposed procedure is illustrated through numerical applications.

3. Extension to the coupled Fluid-Structure system

The purpose is to present a specific method of calculation of the frequencies and the modes of the preceding structure immersed into an incompressible fluid at rest: the state of the fluid is characterized by its field of pressions p. The equations of the coupled system have the form (Wang and Bathe, 1997):

$$\text{Structure} \quad : \quad M\ddot{U} + KU = Lp \tag{16}$$

$$\text{Fluid} \quad : \quad Hp = -\rho_F L^t \ddot{U} \tag{17}$$

3.1 Modal synthesis. Application to the coupled system

We use an analogous approach involving the partition of the system in repetitive subsystems: the cyclic system is decomposed in NS identical subsystems having the form of circular sectors. Each subsystem consists of a solid domain and a fluid domain. Coupling arises through the solid/fluid interface. The internal movements may be described by the superposition of dynamic modes with fixed interfaces and static modes of connection (Olsen and Bathe, 1985):

$$U_i = \Phi_c U_c + \Phi_{Hy} q \tag{18}$$

where Φ_c is the matrix of the static modes, U_c is the vector of the movements in the outline, Φ_{Hy} is the matrix of n_j first hydro-elastic modes with fixed interfaces, q is the vector of n_j hydro-elastic modal variable of the structure.

The internal pressures of the fluid may be described by superposing dynamic modes with interface fixed and static modes:

$$p_i = \Psi_c p_c + \Psi_{R,j} r_j \tag{19}$$

Ψ_c is the matrix of connection between the fluid modes connection; p_c are the boundary components (left and right) of the pressures applied to the cell, $\Psi_{R,j}$ is the matrix of the n_j first Ritz modes with a fixed interface, r_j is the vector formed by the n_j fluid modal variables.

3.2 Application of the method of cyclic symmetry groups.

The phase shift between two sectors is:

$$\alpha_n = \frac{2\pi}{NS}n \quad , \quad \alpha_n \in [-\pi, \pi] \quad .$$

From the theory of the linear representations of symmetry groups (El hami, 2000), we have for each α_n fixed and for the substructure number ℓ :

$$U_\ell = (U_{cn})_I^R \cos((\ell-1)\alpha_n) + (U_{sn})_I^R \sin((\ell-1)\alpha_n) \qquad (20)$$

$$p_\ell = (p_{cn})_I^R \cos((\ell-1)\alpha_n) + (p_{sn})_I^R \sin((\ell-1)\alpha_n) \qquad (21)$$

U_{cn}, U_{sn} , p_{cn}, p_{sn} are given by Eqs. (8) .

These relations determine the movements of all the structure and the field of pressure of the fluid from the values of a single reference sector. The eigenmodes of the whole structure are obtained for every α_n by Eqs (15).

3.3 Summary of the method.

The method of calculation of the eigenfrequencies and eigenmodes of vibration of the coupled cyclic system is summarized as follows:

1) The analysis of the complete system formed by NS identical sectors reduces to the analysis of a single basic sector containing both fluid and structure separated by their interface.
2) The basic sector is discretized by using FEM. Subdomain decomposition is eventually applied to the single basic sector.
4) The static modes of both fluid and structure are determined.
5) The modes of the basic sector are determined.
6) The method of the representations of the finite groups (El Hami,A , 2000) is applied in order to get a representation of the whole structure.
7) The eigenmodes of the whole structure are constructed.

4. Experimental measurement of eigenmodes and eigenfrequencies by electronic holography

In order to get detailed experimental data about eigenmodes and eigenfrequencies without disturbing the specimen we decided to use a full-field, non-contact measurement technique. Such a technique, well adapted to the metrological constraints belongs to the electronic speckle pattern interferometry (ESPI) family. Since the vibrations are mostly out-of-plane and have small amplitudes (in the micrometer range), the particular technique having been used was electronic holography (Fig. 1).
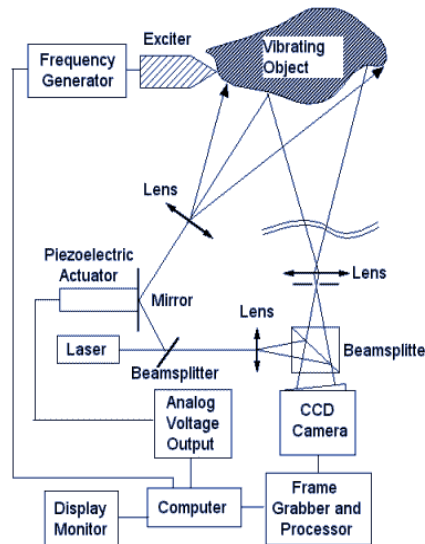
Figure 1. Electronic holography system

In the "classical" method of time-average electronic holography described by (Vikhagen, 1989) four successive frames acquired by the camera are used to produce a fringe pattern, representing the object covered by alternate bright and dark fringes. The fringes are loci of equal values of the projection of the local vibration amplitude on the local sensitivity vector of the setup. They may roughly be considered as loci of iso-amplitude of vibration. The fringe function decribing the fringe pattern is the absolute value of the zero-order, first kind Bessel function of argument proportional to the vibration amplitude, so the expression of the fringe pattern produced by the image processor and displayed by the monitor is.

$$I_{TAV} = B(x, y)\left|J_0\left[\varphi_v(x, y)\right]\right|$$

(24)

where *B(x,y)* represents the speckled image of the object in its equilibrium position, $J_0(z)$ is the zero-order, first kind Bessel function of argument *z* and the deterministic phase term $\varphi_v(x, y)$ is a function of the out-of-plane vibration amplitude *d(x,y)* of the object point imaged at *(x,y)*. It is given by the approximate relation:

$$\varphi_v(x, y) = \frac{4\pi}{\lambda} d(x, y)$$

(25)

where   is the laser light.wavelength.

Bright fringes, whose intensity is decreasing with the fringe order n, are given by the successive maxima of eq. (24), which are:

$$d = 0, \frac{5\lambda}{16}, \frac{9\lambda}{16}, \frac{13\lambda}{16}, \frac{17\lambda}{16}, ..., \frac{(4n+1)\lambda}{16} \qquad n = 1, 2, 3, ...$$

(26)

and dark fringes of zero intensity, corresponding to the minima of eq. (1), appear for:

$$d = \frac{3\lambda}{16}, \frac{7\lambda}{16}, \frac{11\lambda}{16}, \frac{15\lambda}{16}, ..., \frac{(4n-1)\lambda}{16} \qquad n = 1, 2, 3, ...$$

(27)

The widespread use of the time-averaged method is due to its real-time character, but also to the other characteristics, such as the indepence of its sensitivity with respect to frequency. As the fringe contrast strongly decreases with fringe order and because of its speckle noise, if the complete full-field of amplitudes is required quantitatively, other methods may be used such as recording phase interferograms as described by (Pryputniewicz and Stetson, 1989) or quasi-binary interferograms as described by (Borza, 2002).

The quasi-binary electronic holography uses two 4-frames buckets; the first one corresponds to the stationary object and the second one to the vibrating one. The use of these primary data fields allows obtaining a fringe pattern of high contrast, containing essentially only two intensity levels, well separated on the histogram of the fringe pattern. The bright fringes are loci of all object points where the zero-order, first kind Bessel function of argument proportional to the vibration amplitude is positive. The dark fringes are loci of all points where the Bessel function is negative. The number of fringes is halved with respect to the time-averaged method, so the measurement range is doubled.

These two methods use algorithms allow obtaining fringe patterns given respectively by:

$$I_{PI} = A\varphi_v\big|_{\text{mod}ulo\ 2\pi}$$

(28)

(*A* being a constant) in the case of the phase interferograms, and by:

$$I_{QB} = \Delta\varphi_{o-r} + \frac{sign(J_0(\varphi_v)) + 1}{2} \times \pi \,.$$

(29)

($\Delta\varphi_{o-r}$ being a constant or slowly varying factor) in the case of quasi-binary interferograms.

The laser used in measurements was a frequency-doubled CW YAG laser of wavelength 532 nm. During the vibration testing with acoustic excitation, the exciter was a loudspeaker placed behind the object. The excitation sine signal of arbitrary frequency was produced by a standard arbitrary waveform generator, followed by an audio amplifier adapted to the loudspeakers impedance. The detection of resonant frequencies was done by looking at the object image on the monitor while slowly varying the excitation frequency. When approaching a resonance, the fringe pattern starts covering the object; the number of fringes is maximum (and the width of nodal lines is a minimum) at resonance. If more than a single mode responds for a particular frequency, the nodal lines not only become thiner and thiner while approaching the frequency of resonance, but they also change their orientations or shapes, according to the influence of each mode in the total response of the object.. This allows identifying these situations and eventually avoiding mode coupling by adjusting the position of the loudspeaker.

Figure 2 presents some of the most important experimentally determined modes along with their corresponding frequencies.

| 209 Hz | 226 Hz | 332 Hz | 334 Hz |
| 850 Hz | 1567 Hz | 1496 Hz | 1882 Hz |
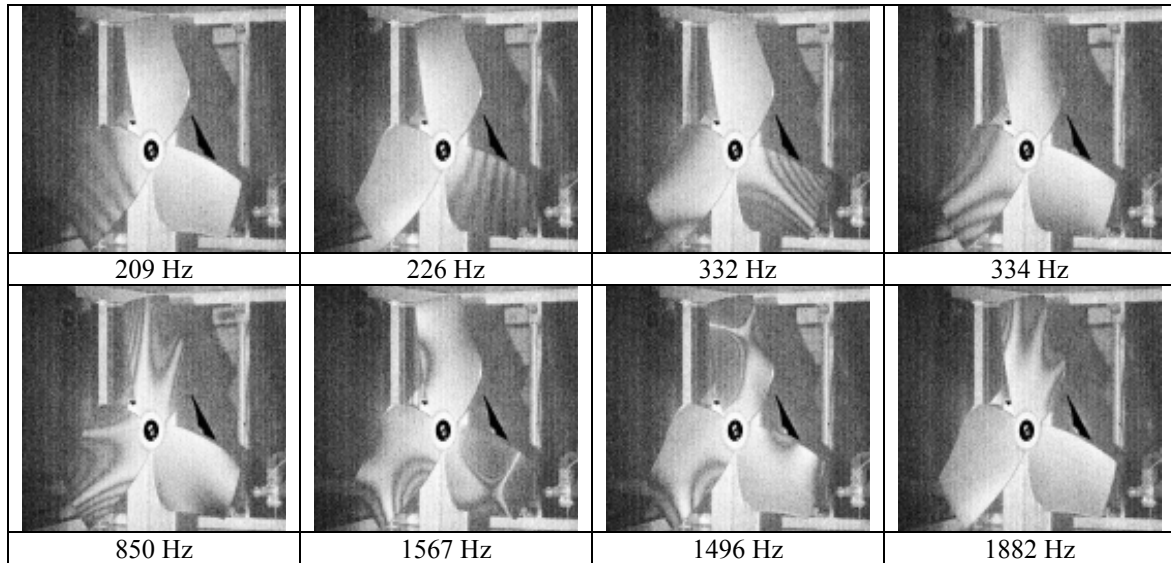
Figure 2. Some of the vibration amplitude distributions and their resonance frequencies

5. Simulation

The problem considered here is the determination of the eigenmodes of the propeller.
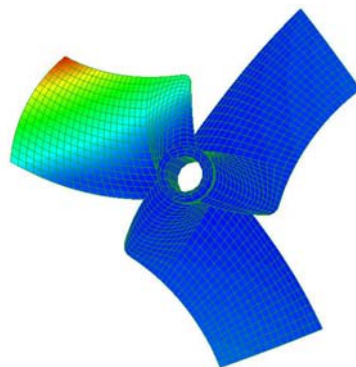
Figure 3. Deformed mesh of the propeller

The base cell (1/3 of global structure) is modeled by quadratic elements with six DOF per node . A deformed mesh is represented in Fig.3. A comparison with the experimental results obtained in the laboratory is given in Table 1.

Table 1. Comparison between numerical and experimental results

Numerical (Hz) in air f_{num}	Experimental (Hz) in air f_{exp}	$(f_{exp} - f_{num})/f_{exp}$ (%)	Numerical (Hz) in water
209	209	—	092
248	226	9.7	124
261	---	---	--
351.4	332	6	193.3
363	334	8.7	233
743	---	---	--
840	850	-1.2	525
1511.3	1496	1.02	983.2
1571	1567	0.25	1133.2
1889	1882	0.37	1316.5
1974.4	1901	3.9	1467
2070	---	----	1533.2

We notice a relative concordance between numerically predicted and experimentally measured frequencies (electronic holography): the proposed approach has led to acceptable results concerning the nodal displacements and eigenfrequencies for out-of-plane modes.

6. Conclusion

A method for structural analysis of a cyclically symmetric structure immersed in a fluid at rest has been presented. The proposed method saves memory requirements and CPU cost by reducing the number of DOF to be considered. It is based upon the representation of finite symmetry groups. The experimental comparison has shown that the approximations introduced are acceptable and lead to good results. Futur work concern the extension to quasi-symmetric problems.

7. References

Borza, D., 2002, "A new Interferometric Method for Vibration Measurement by Electronic Holography", Experimental Mechanics, vol. 42, No. 4, pp. 432-438.

Chan, S.L , 1996, "On the possible application of group representation boundary value and eigenvalue problems of certain domains without classical symmetry", Angew. Math. Phys. 27, pp. 553-561, 563-572, 840-851.

Corn, S., Piranda, J. and Bouhaddi, N. (2000). "Simplification of finite element models for structures havig a beam-like behavior," Journal of Sound and Vibration, 232(2), pp. 331-354.

Craig R.R. J. and Bampton M.C.C. (1968). American Institute of Aeronautics and Astronautics journal, 6, pp. 1313-1319, Coupling of substructure for dynamic analysis.

El hami.A, 2000,Contribution à la résolution des systèmes de grande dimension et à l'analyse probabiliste d'un problème de contact en mécanique des structures". HDR, à l'université de Franche-Comté, soutenue le 13/1/2000.

El hami.A and RADI.B, 1996, Some Decomposition Methods in the Analysis of repetitive structures; Computers & structures, vol 58, N°5, pp 973-980.

El hami.A and RADI.B, 2003, Numerical simulation of a piezoelectric engine with progressive wave via a reliability technique, Proceeding SCSC´03.

Enevoldsen, I., and Sorensen, J.D., 1994, "Reliability-based optimization in structural engineering," Structural Safety, 15, pp. 169-196.

Grandhi, R.V., Wang L., 1998, Reliability-based structural optimization using improved two-point adaptive nonlinear approximations. Finite Elements in Analysis and Design 29, pp. 35-48.

Moro.T, El hami.A, El moudni., 2002, Reliability analysis of a mechanical contact between solids, International Journal of Probabilistic Engineering Mechanics, Vol 17 n°3, pp. 227-232.

Olsen.L.G, Bathe.K.J., 1985, Analysis of fluid-structures interactions. A direct symmetric coupled formulation based on the fluid velocity potential", computer and structures, vol 21, pp. 21-32.

Pryputniewicz, R. J., Stetson, K. A., 1989, "Measurement of vibration patterns using electro-optic holography", Proc. SPIE, 1162, pp. 456-67.

Vikhagen, E., 1989, "Vibration measurement using phase shifting TV-holography and digital image processing ", Opt.Commun; Vol. 69, 3, pp. 214-218.

Wang.X, Bathe.K.J., 1997, Displacement /pressure based mixed finite element formulations for acoustic fluid-structure interaction problems" Int. Jour. for Num. Meth. Ing., vol. 40, pp. 2001-2017.

8. Responsibility notice

The authors are the only responsible for the printed material included in this paper.